Biomaterials 32 (2011) 6351–6361

Contents lists available at ScienceDirect

Biomaterials

journal homepage: www.elsevier.com/locate/biomaterials

Quantification of *in vitro* and *in vivo* angiogenesis stimulated by ovine forestomach matrix biomaterial

Sharleen M. Irvine [a,b], Juliet Cayzer [c], Elise M. Todd [a], Stan Lun [a], Evan W. Floden [a], Leonardo Negron [a], James N. Fisher [a], Sandi G. Dempsey [a], Alan Alexander [c], Michael C. Hill [e], Annalee O'Rouke [f], Sarah P. Gunningham [d], Cameron Knight [g], Paul F. Davis [b,f], Brian R. Ward [a], Barnaby C.H. May [a,*]

[a] *Mesynthes Limited, P.O. Box 31311, Lower Hutt 5040, New Zealand*
[b] *Department of Medicine, University of Otago, Wellington, P.O. Box 7343, Wellington South 6242, New Zealand*
[c] *Estendart Limited, Private Bag 11222, Palmerston North 4442, New Zealand*
[d] *Christchurch Angiogenesis and Cancer Research Group, University of Otago, PO Box 4345, Christchurch 8011, New Zealand*
[e] *Waikato District Health Board, Private Bag 3200, Hamilton 3240, New Zealand*
[f] *Trinity Bioactives Limited, P.O. Box 15135, Wellington 6243, New Zealand*
[g] *Institute of Veterinary, Animal and Biomedical Sciences, Private Bag 11222, Palmerston North 4442, New Zealand*

ARTICLE INFO

Article history:
Received 27 April 2011
Accepted 10 May 2011
Available online 12 June 2011

Keywords:
Angiogenesis
Animal model
Bioactivity
ECM (extracellular matrix)
Scaffold
Growth factors

ABSTRACT

Ovine forestomach matrix (OFM) biomaterial acts as a biomimetic of native extracellular matrix (ECM) by providing structural and functional cues to orchestrate cell activity during tissue regeneration. The ordered collagen matrix of the biomaterial is supplemented with secondary ECM-associated macromolecules that function in cell adhesion, migration and communication. As angiogenesis and vasculogenesis are critical processes during tissue regeneration we sought to quantify the angiogenic properties of the OFM biomaterial. *In vitro* studies demonstrated that soluble OFM components stimulated human umbilical vein endothelial cell (HUVEC) migration and increased vascular sprouting from an aorta. Blood vessel density and branch points increased in response to OFM in an *ex ovo* chicken chorioallantoic membrane (CAM) assay. The OFM biomaterial was shown to undergo remodeling in a porcine full-thickness excisional model and gave rise to significantly more blood vessels than wounds treated with small intestinal submucosa decellularized ECM or untreated wounds.

1. Introduction

The success of biomaterials as templates for tissue regeneration is mainly dictated by their ability to rapidly vascularize and therefore allow for the efficient delivery of requisite cellular nutrients during regeneration. The formation of vasculature also enables complete cellular infiltration of the graft as autologous cells migrate from the periphery of the implant site into the graft materials. As blood supply to the graft mediates long-term healing, well-vascularizing biomaterials generally have better healing outcomes [1]. Additionally, a robust blood supply is thought to reduce infection by facilitating the egress of microbes from the site and allowing complete infiltration of immune components [2,3].

The revascularization of biomaterials comprising decellularized extracellular matrices (dECM), for example, human allogenic dermis (HAD, Alloderm®) and porcine small intestinal submucosa (SIS, SurgiSIS®; OaSIS®) has been demonstrated clinically [4,5]. The relatively rapid vascularization of these biomaterials has driven their clinical uptake in a number of applications including herniaplasty, breast reconstruction, tendon repair and dural repair [6]. dECM biomaterials are produced from intact tissues using processes that decellularize the tissue ECM whilst retaining the native structural features, including an ordered collagen microarchitecture and residual vascular channels. In addition to providing native architecture to support cell adhesion and migration, these biomaterials additionally retain important secondary molecules that mediate cellular interactions including growth factors, glycosaminoglycans, and adhesive molecules such as laminin and collagen IV [7,8].Together these structural, adhesive and signaling molecules work in concert to mimic native ECM. As biomimetics of normal tissue ECM, dECM-based biomaterials undergo constructive remodeling in a process that recapitulates features of normal tissue turn-over [9]. The exact mechanism by which dECM-based biomaterials act to regulate migration, proliferation and differentiation of endothelial cells during the regenerative process is not known in detail. The response may be

* Corresponding author.
E-mail address: barnaby.may@mesynthes.com (B.C.H. May).

0142-9612/$ – see front matter © 2011 Elsevier Ltd. All rights reserved.
doi:10.1016/j.biomaterials.2011.05.040

attributed to angiogenic growth factors, particularly, fibroblast growth factor 2 (FGF2), vascular endothelial growth factor (VEGF), platelet derived growth factor (PDGF) and hyaluronic acid (HA) that are known to be present in dECM-based biomaterials [10–13]. Additionally, it has been demonstrated that bioactive degradation products from dECMs are capable of recruiting endothelial progenitor cells [14,15].

dECM biomaterials have been prepared from a number of different allogenic and xenogenic source tissues, including human cadaveric dermis, porcine urinary bladder and bovine pericardium [7]. OFM was developed to overcome some of the size limitations and cultural objections to existing commercially available dECM-based biomaterials. OFM is prepared from the propria submucosa of ovine forestomach tissue using detergent-based processes to delaminate and decellularize the tissue.

Structural studies have shown that the OFM biomaterial is relatively strong and elastic [16] and retains the complex collagen architecture of native tissue ECM [8]. OFM additionally retains secondary ECM-associated molecules, including FGF2, heparan sulfate, and HA, as well as remnant basement membrane components associated with the forestomach luminal surface and endothelial basement membranes [8]. Given that OFM retains the requisite structural and functional components of native ECM the ability of this biomaterial to mediate endothelial migration and angiogenesis was quantified both *in vitro* and *in vivo*. Furthermore, this study compares the angiogenic potential of OFM with that of chemically cross linked OFM, dECM derived from porcine small intestinal submucosa (SIS) and a collagen-based wound dressing composed of bovine collagen (type I) and oxidized regenerated cellulose (Promogran™).

2. Materials and methods

2.1. General

All experiments were conducted at room temperature unless otherwise indicated. OFM was prepared from ovine forestomach propria submucosa as defined in Lun et al., and terminally sterilized (ethylene oxide) according to established procedures [8]. OFM biomaterial was cross linked to give OFM-X using 1-ethyl-3-(3-dimethylaminopropyl) carbodiimide and *N*-hydroxysuccinamide according to Floden et al. [16]. dECM from porcine SIS (OaSIS®) was sourced from Healthpoint Limited (Texas, USA). Collagen-containing wound dressing, Promogran™ (PG), was sourced from Systagenix Limited (West Sussex – UK). OFM, OFM-X, SIS and PG were powdered to ~200 μm using an Ultra-centrifugal Mill ZM 200 (Retsch – Haan, Germany). HUVEC were isolated from umbilical cord veins according to established procedures [17], after obtaining informed consent under appropriate ethical approval. HUVEC cells were maintained in M199 media (Invitrogen – CA, USA) containing microvascular growth supplement (MVGS, Invitrogen) and 10% fetal bovine serum (FBS, Invitrogen) at 37 °C in an atmosphere of 5% CO_2. All HUVEC were cultured in M199 with MVGS and 2% FBS (M199-2). Rat aortas were maintained in MCDB-131 media (Invitrogen) at 37 °C and 3% CO_2. Ethical approval for animal surgery was obtained from the Kaiawhina Animal Ethics Committee (Palmerston North, New Zealand) and the Wellington School of Medicine Animal Ethics Committee (Wellington, New Zealand). Standard aseptic technique was used for all tissue culture and *in vivo* surgeries.

2.2. Endothelial cell migration and proliferation assay

HUVEC cells were seeded in a poly-L-lysine coated 96-well-plate (20,000 cells/well; Jet Biofil – China) at passage five and grown to 80% confluency over 24 h. Where required, cells were incubated with mitomycin C (5 ng/mL in dH_2O; Sigma Aldrich – MI, USA) for 2 h at 37 °C and 5% CO_2 to inhibit cell proliferation [18]. A ~1 mm scratch running through the middle of each well was created in the monolayer using the end of a p10 pipette tip. The cell monolayer was washed three times with M199-2 (200 μL) to remove cellular debris. Test extracts were prepared by adding powdered OFM, SIS, OFM-X and PG to PBS at 50 and 100 mg/mL, and incubating for 24 h at 37 °C with gentle shaking. The samples were centrifuged (13 k rpm, 5 min), and the supernatant filter sterilized (0.22 μm). The protein concentrations of the extracts were determined using the bicinchoninic acid (BCA) protein assay (Pierce – IL, USA), according to the manufacturer's instructions. Test solutions (200 μL) were diluted 1:3 in M199-2 prior to use. Cells treated with recombinant $VEGF_{121}$ (5 ng/mL in PBS; Peprotech – NJ, USA) and PBS (Invitrogen) served as positive and negative controls, respectively. Wells were imaged at 10× immediately after dosing, then at 4 and 8 h using an IX51 inverted microscope (Olympus – Tokyo, Japan) fitted with a Colorview III camera (Olympus). One frame was captured per well, such that the scratch aligned vertically through the image. Infill of the scratch was determined by comparing the total area of the scratched cell monolayer (pixels) at dosing and then after 4 and 8 h incubation. The area of the monolayer was measured using ImageJ (National Institute of Health – MD, USA) and expressed in megapixels. Statistical significance was calculated using a two-way ANOVA and Bonferroni post-hoc tests (GraphPad Prism – CA, USA).

2.3. Aortic ring assay

The aortic ring assay was conducted with modifications to an existing procedure [19]. A single Lewis female rat (6–8 weeks old) was euthanized using CO_2 and the aorta harvested and transferred to sterile culture medium (10 mL). The tunica adventitia of the aorta was dissected away with the aid of a dissection microscope (Olympus SZ60). The aorta was cut into rings approximately 2 mm in length then further cleaned by microdissection before being pre-incubated overnight in media at 37 °C. Test samples were prepared using either a powdered sample of OFM, or a media extract of powdered OFM. The former was prepared by rehydrating powdered OFM in media (0.2 mg/mL) for 5 min and vortexing to ensure uniform distribution of the test article, prior to the addition of fibrinogen (Sigma) to a final concentration of 3 mg/mL. OFM extracts were prepared by adding powdered OFM at 10 mg/mL to MCDB-131 media, and incubating for 24 h at 37 °C with gentle shaking. The samples were centrifuged (13 k rpm, 5 min), and the supernatant filter sterilized (0.22 μm). To this media extraction, fibrinogen was added to a final concentration of 3 mg/mL. Thrombin (Serva, Heidelberg, Germany) was added to all test samples to give a final concentration of 1 U/mL. Each of the test samples (0.5 mL) in the fibrinogen-thrombin solution was transferred to separate wells of a 24-well-plate. A single aortic ring was placed in the center of the setting gel and left to set for 45 min. A further 0.5 mL of the test solution was transferred so as to cover the aortic ring. Once the gels were completely set, media (1.5 mL) was added to completely cover the top of each gel. Gels treated with recombinant $VEGF_{121}$ served as positive controls, whereby the fibrin gel was covered with media (1.5 mL) previously supplemented with $VEGF_{121}$ (10 ng/mL). Aortic rings placed in non-supplemented gels were used as negative controls. The plate was incubated at 37 °C and imaged at days 3, 5, and 7 at 4× magnification using an Olympus CK2 microscope fitted with an Olympus UC30 camera. Using ImageJ, the edges of the vessels in the microphotographs were identified and an image mask was created to clearly identify microvasculature. Using this mask, the area of microvasculature was quantified and expressed as pixels. A two-way ANOVA and Bonferroni post-hoc tests (GraphPad Prism) were used to show significance relative to untreated controls.

2.4. Chicken CAM assay

Fertile chicken eggs (Hyline Brown, Golden Coast Commercial – Levin, New Zealand) were wiped clean with dH_2O and incubated at 38.5 °C/~75% RH for 72 h. Eggs were wiped with 70% ethanol, and then aseptically cracked into sterile Petri dishes (20 mm high, 100 mm diameter; Labserv – Auckland, New Zealand). Penicillin/streptomycin (200 μL, 10,000 U; 10,000 μg; Invitrogen) was injected into the albumin to protect the culture from contamination. *Ex ovo* cultures were returned to the incubator (37.5 °C/85–90% RH) for 84 h (3.5 days). Up to six sterile polytetrafluoroethylene (PTFE) rings (12 mm I.D.; Seal Imports – Hamilton, New Zealand) were placed onto each membrane so as to surround the major blood vessel branch points, with care being taken not to place two rings on the same major blood vessel. Each ring was gently pressed down to avoid movement of the ring during dosing and incubation. Powdered biomaterials were extracted and the protein concentration of the extracts determined, as described above. The interior of each ring was dosed with 20 μL of the test extracts, PBS or $VEGF_{121}$ (1 μg/mL solution in PBS, Invitrogen). In each case the solutions were gently spread over the surface of the CAM contained within the PTFE ring. The location of each test sample was varied so as to remove any bias between individual CAM cultures. The cultures were incubated for a further three days and each ring was digitally imaged at days 0, 1, 2 and 3 post dosing using an ES15 digital camera (Samsung – Korea). The total area of blood vessels (pixels) within each ring was quantified from the digital images using ImageJ by deconvoluting the image, such that the red blood vessels could be separated from the surrounding image. Results were expressed as a percentage increase in the area of vasculature relative to day 0. Additionally, the vessel branch points within each ring were manually counted from inspection of the digital images. Results were expressed as a percentage increase in branch points relative to day 0. Two-way ANOVA and Bonferroni post-hoc tests (GraphPad Prism) were used to show significance relative to untreated controls.

2.5. Porcine full-thickness excisional model

Disease-free Landrace female pigs ($n = 5$, 15–20 kg) were treated with a Fentanyl transdermal patch delivering 75 μg/h, (Duragesic, Ortho-McNeil-Janssen Pharmaceuticals, Inc – NJ, USA) one day prior to intramuscular administration of ketamine (13 mg/kg; Phoenix Pharmaceuticals Inc – NJ, USA) and midazolam

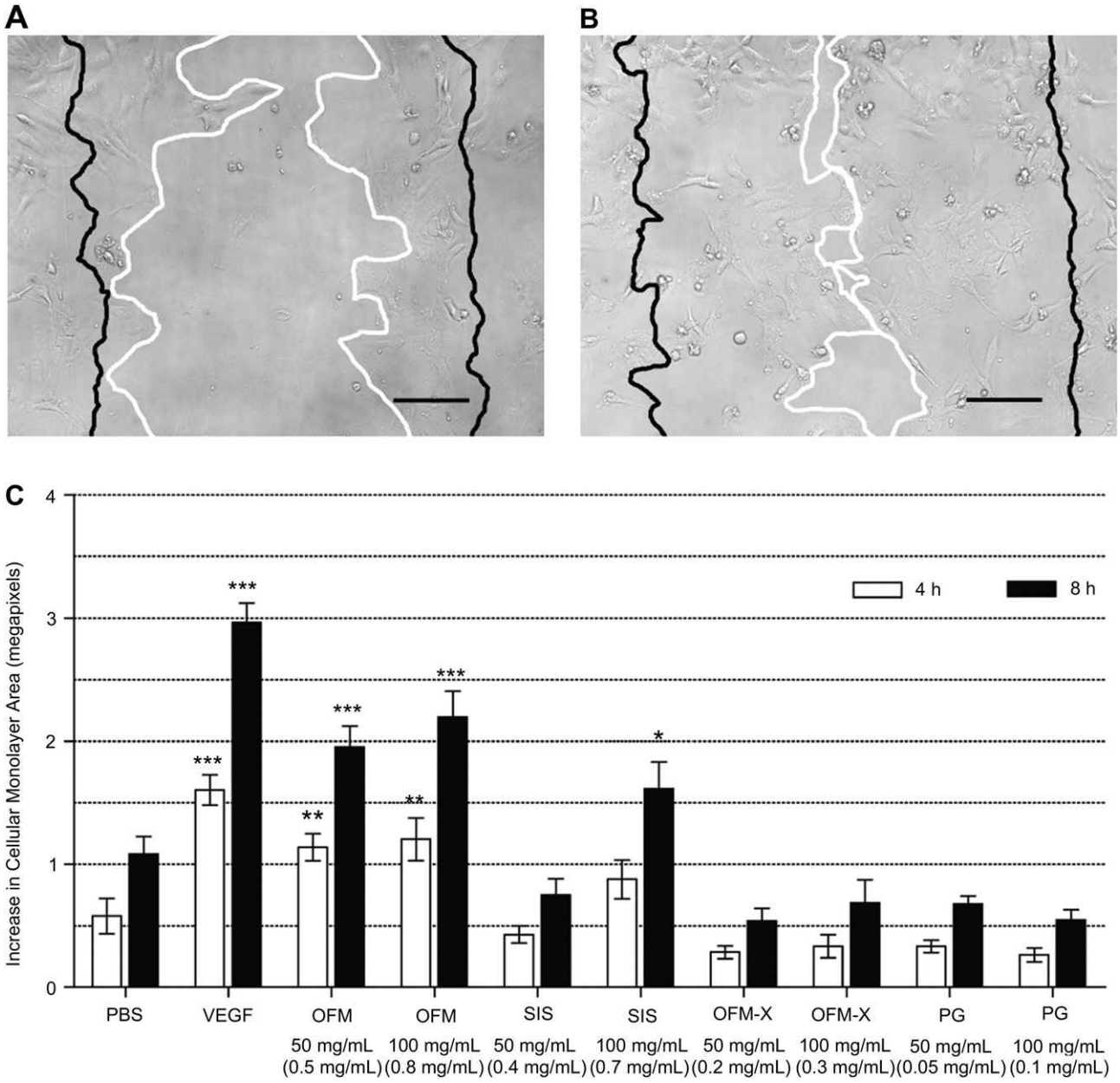

Fig. 1. Bioactivity of biomaterials in the HUVEC cell migration and proliferation assay. A. Representative images of changes to the denuded cell monolayer following PBS treatment and B. Representative images of changes to the denuded cell monolayer after incubation with an OFM extract (0.8 mg/mL). Margins of the monolayer at $t = 0$ h are depicted as a black line while margins of the monolayer at $t = 8$ h are indicated by the white line. Scale bar = 100 μm C. Quantification of the extent of changes to the area of the cell monolayer (megapixels) due to proliferation and migration relative to $t = 0$. Concentration indicated in brackets is the extract protein concentration prior to a 1:3 dilution into media. Error bars represent SEM from triplicate experiments. '*', '**' and '***' = $P < 0.05$, $P < 0.01$ and $P < 0.001$ respectively, using two-way ANOVA and Bonferroni post-hoc tests relative to the untreated controls.

(1.5 mg/kg; Hyponovel, Roche – Switzerland). Anesthesia (1 mg/kg Propofol; Repose; Norbrook – Australia) was then administered to intubate the animals and anesthesia was maintained with isoflurane (Attane; Bomac – New Zealand) in oxygen delivered either via endotracheal tube, or face mask. Animals were positioned in ventral recumbency and the hair of the dorsal region was removed from the base of the neck to the caudal lumbar area and laterally 20 cm either side of the mid-line. Morphine (20 μg/kg; Hameln Pharmaceuticals – Germany) was given during anesthesia, and the animals were treated prophylactically with penicillin (Tripen LA, 6.25 mg/kg; Ethical Agents – New Zealand). Preparation of the surgical site was performed using 0.5% chlorhexidine (Microshield 4%; Johnson and Johnson – NJ, USA) and 70% ethanol, and the excisional sites marked with a surgical pen. The cranial wound sites were positioned immediately posterior to the dorsal shoulder blades and wounds extended caudally towards the sacrum. In total 20 wounds (5 rows of 4 wounds) were made in the skin of each animal, separated from one another by 30 mm. Using a 20 mm sterile biopsy punch (Shoney Scientific – India), each wound was made perpendicular to the surface of the skin penetrating through the dermal layer and into the fatty subcutaneous layer. Tissue was separated from the underlying muscle using a scalpel blade. Dry matrix (OFM or SIS) was applied to the sites and rehydrated *in situ* with sterile saline (approx. 5 mL; Fresenius Kabi – New Zealand). Either OFM or SIS was used to treat 25 wounds each over five different animals. Untreated wounds ($n = 25$) were included as negative controls and a further 25 excisional sites were excluded from the study. The location of the treatments was varied between each animal so as to remove any positional bias due to the location of the surgical site. Hydrating gel (Intrasite, 2 mL; Smith and Nephew – UK) was aseptically applied to cover each wound and the wounds dressed with paraffin gauze (Mepitel; Mölnlycke – Sweden), and cotton gauze (Paranet; Vernon Carus – UK). The dressings were held in place using adhesive wrap (Vetwrap; 3M – MN, USA and Tensoplast; BSN Medical – Germany) and finally a stockinette tube (Surgifix; BSN Medical). Each animal was extubated and monitored to ensure complete recovery from the anesthetic. Dressings were changed as required and the animals monitored daily by a veterinarian or trained animal care technicians. At days 3, 7, 14, and 28 post-surgery, excisional sites from each treatment group (i.e OFM, SIS

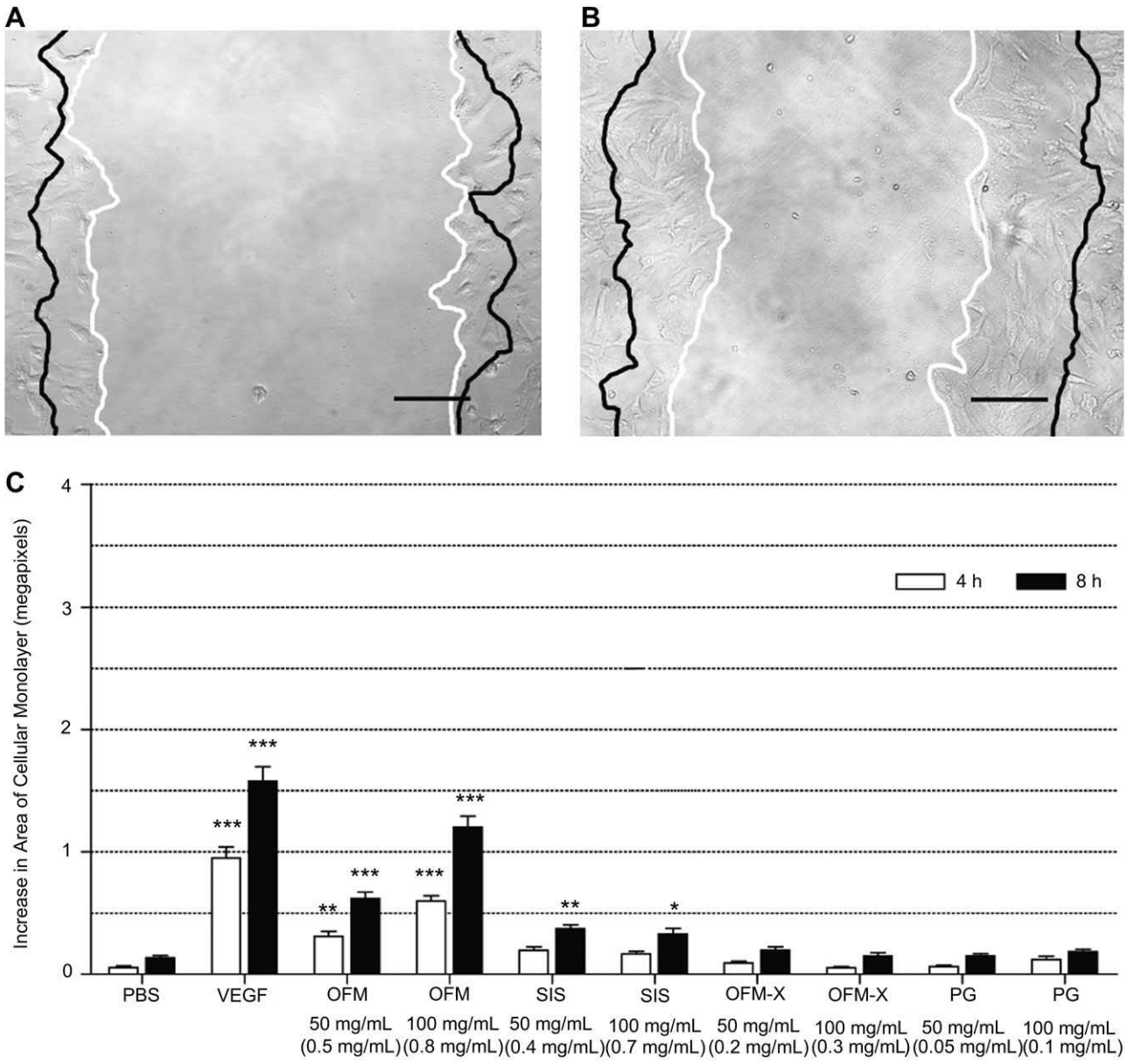

Fig. 2. Bioactivity of biomaterials in the HUVEC migration assay. A. Representative images of cell migration in PBS-treated wells and B. Representative images of cell migration in wells treated with 0.8 mg/mL of OFM extract. Margins of the monolayer at $t = 0$ h are depicted as a black line whereas margins at $t = 8$ h are indicated by the white line. Scale bar = 100 μm. C. Quantification of the total area of the cell monolayer (megapixels) due to migration relative to $t = 0$. Concentration indicated in brackets is the extract protein concentration prior to a 1:3 dilution into media. Error bars represent SEM from triplicate experiments. '*', '**' and '***' = $P < 0.05$, $P < 0.01$ and $P < 0.001$ respectively, using two-way ANOVA and Bonferroni post-hoc tests relative to the untreated controls.

and untreated) were biopsied such that five wounds from each treatment were sampled. Each animal was given analgesic and anesthesia as described above but without the Fentanyl patch. Using a scalpel the entire site was excised by making an elliptical shaped incision taking in the entire site and a portion of surrounding skin. Opposing edges of the excisional site were closed using monofilament nylon suture (Ethilon, size 3/0; Johnson and Johnson – NJ, USA). The wound was dressed according to the method described previously. The excised tissue was rinsed quickly in sterile saline to remove blood and debris, and immediately fixed in 10% v/v formalin in PBS. Animals were humanely euthanized by captive bolt followed by exsanguination at day 42 and the remaining excisional sites removed and formalin-fixed as above.

2.6. Histology

Formalin-fixed (10% v/v formalin in PBS; Sigma) tissues were paraffin-embedded, cut at 5–10 μm using a microtome (HM325, Microm – Germany), then floated onto positively charged slides (Superfrost R Plus, Menzel-Glaser – Germany). Sections were stained with Gomori's trichrome stain according to established procedures [20]. Briefly, sections were placed in Bouins Fluid (picric acid – Sigma) overnight, then iron haematoxylin (Sigma) for 10 min before connective fibers were stained with Gomori's Trichrome stain (Chromotrope 2R, 0.6%; Fast green FCF, 0.3%; phosphotungstic acid, 0.6%; acetic acid 1%; pH 3.4; Sigma) for 15 min. The slides were rinsed in 0.2% acetic acid, then cover-slipped with Eukitt mounting media (Electron Microscopy Services – PA, USA). Sections were visualized at 4× magnification using a BX51 microscope fitted with a DP20 camera (Olympus). Multiple images across the entire section were taken and subsequently the individual frames were 'stitched' together using AnalySIS (Olympus) to create a single 4× image of the entire tissue section. Sections were examined using light microscopy in a blinded fashion by a US board certified veterinary pathologist (C.K.).

2.7. Immunohistochemistry

Formalin-fixed tissues from the animal study were paraffin-embedded, cut and mounted as described above. Slides were left to dry prior to staining. Slides were stained using a Bond Max Autostainer (Vision Biosystems, Australia) and all solutions were sourced from Vision Biosystems, unless otherwise stated. Solutions were dispensed directly onto slides (150 μL) and 1 min incubation in Bond™ Wash Solution was used for all washes. All antibody dilutions were made using Bond™

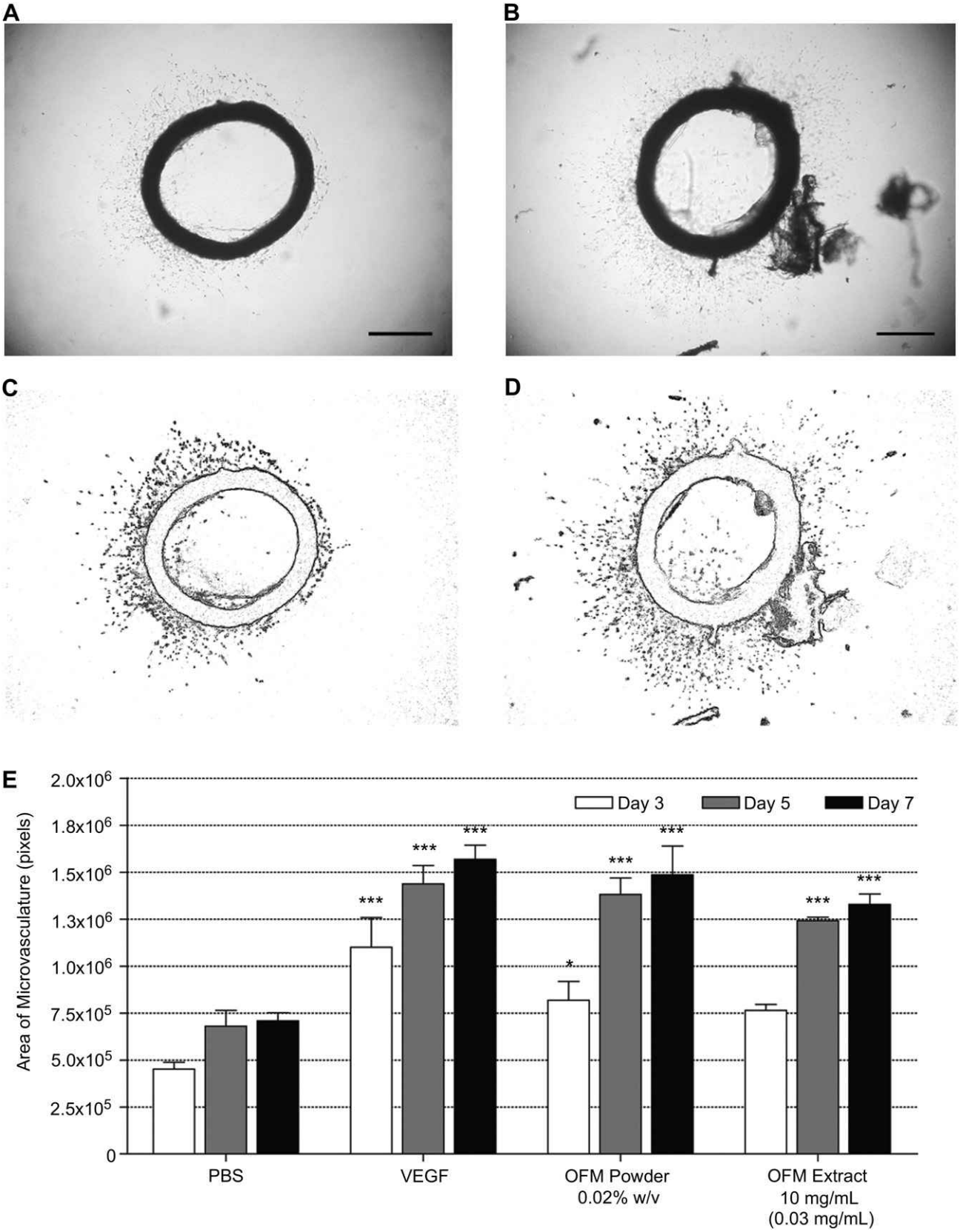

Fig. 3. Representative images of rat aorta at day 7 either A. untreated C. and corresponding mask, or B. in the presence of 0.02% w/v OFM powder D. with mask. OFM particles can been in the periphery of the field. Scale bar = 250 μm. E. Quantification of the increase in microvasculature at the indicated days. At day 0, no microvessels were evident in any samples. Concentration indicated in brackets is the extract protein concentration used to make the fibrin clot. Error bars represent SEM from triplicate samples. '*' and '***' = $P < 0.05$ and $P < 0.001$ respectively, using two-way ANOVA and Bonferroni post-hoc tests relative to the untreated controls.

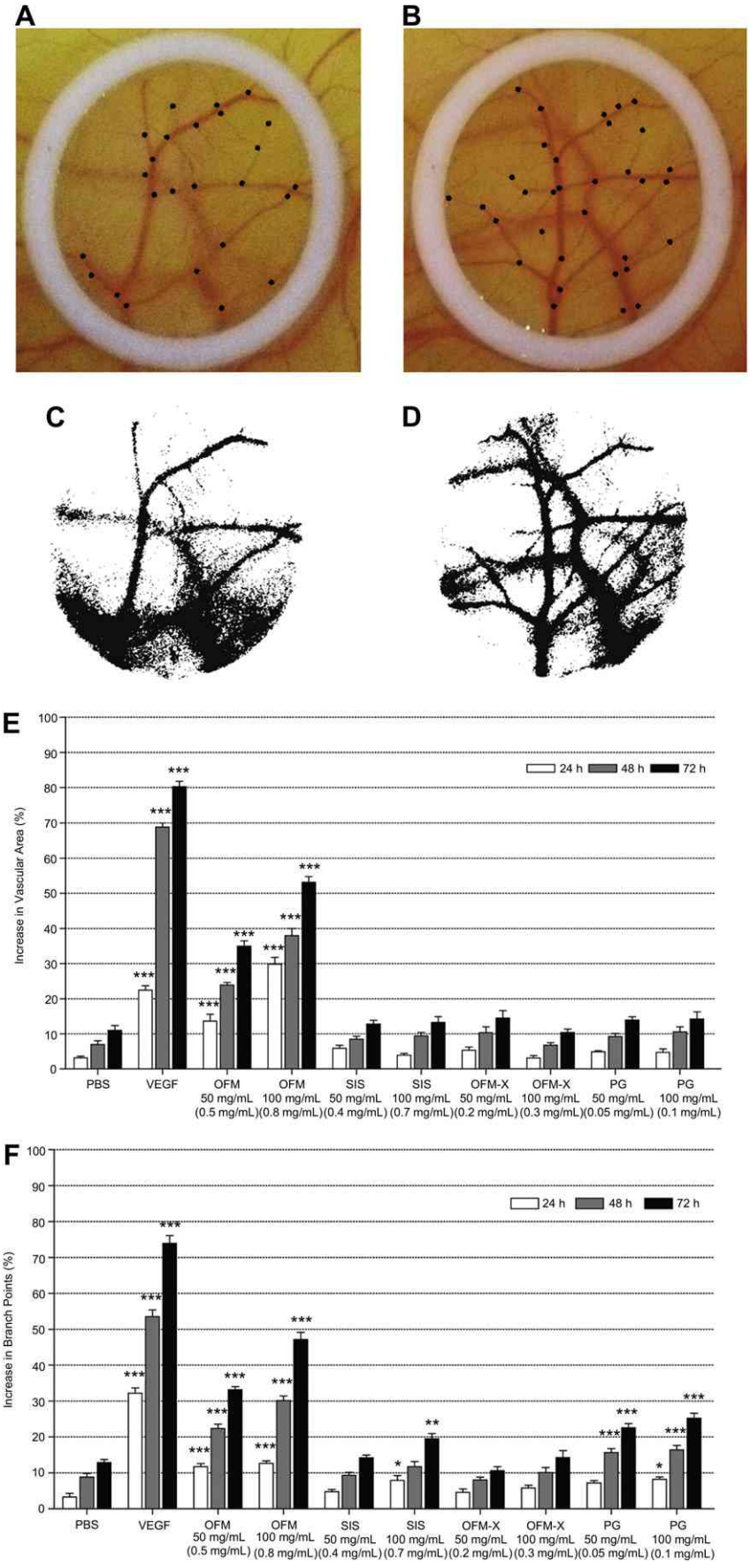
A
B
C
D
E
Increase in Vascular Area (%)
24 h
48 h
72 h
PBS
VEGF
OFM 50 mg/mL (0.5 mg/mL)
OFM 100 mg/mL (0.8 mg/mL)
SIS 50 mg/mL (0.4 mg/mL)
SIS 100 mg/mL (0.7 mg/mL)
OFM-X 50 mg/mL (0.2 mg/mL)
OFM-X 100 mg/mL (0.3 mg/mL)
PG 50 mg/mL (0.05 mg/mL)
PG 100 mg/mL (0.1 mg/mL)
F
Increase in Branch Points (%)

Antibody Diluent. Sections were dewaxed using the Bond™ Dewax solution (3 × 1 min) then rehydrated by incubating in descending concentrations of EtOH for at least 1 min each. Slides were washed (3×) before being subject to heat-induced epitope retrieval. CD34 epitopes were retrieved using Bond™ ER Solution #1, (pH 8.9–9.1) for 20 min. Slides were washed (6×), incubated in Bond™ Peroxidase Blocking Solution (5 min), before being washed (3x) again. Slides were incubated (18 min) with primary antibody (goat anti-porcine CD34, 1:100, RnD Systems – MN, USA), washed (3×), then incubated (10 min) with anti-goat HRP-IgG (DakoCytomation, Denmark). Slides were washed (6×), incubated in Bond™ Post Primary Solution (8 min), washed (3×) then incubated in Bond™ Max Polymer Solution (8 min). Slides were washed (2×) then rinsed with dH_2O (2 min) before incubation with Bond™ Mixed DAB Refine Solution (2 min, 10 min). Slides were rinsed in dH_2O before being counterstained with Mayer's Hemotoxylin and rinsed in dH_2O (4 min), Bond™ Max Solution (1 min) and dH_2O (1 min). Slides were immersed in tap water (30 s) and dehydrated through graded EtOH (3 × 4 min) before being cleared in xylene (2 min) using a Tissue-Tek DRS 2000 Autostainer rack (Sakura – CA, USA). Slides were cover-slipped using a Tissue Tek Glas automated coverslipper (Sakura – CA, USA) and Mounting Medium 24 (Surgipath – IL, USA). Immunostained slides were visualized at 10× magnification and digitally imaged using a CX31 light microscope fitted with a DP12 camera and DP12 capture software (Olympus). For CD34 analysis, four images were taken from the regenerating dermal layer (days 7, 14, 28 and 42). The centre of the wound bed was estimated using a light microscope and images were selected and captured from above, below and either side of the central point. The area contained within the four image frames was approximately 11% of the total wound bed. Using ImageJ (NIH) images were processed to quantify the number of positively-stained cells per frame. Firstly, images were deconvoluted to separate the brown DAB staining from the other color components present in the image, and then background staining was subtracted via the threshold function. The monochrome brown image was filtered to remove smaller non-specifically stained particles (<300 μm^2) and an image mask was created to clearly identify clusters. CD34-positive vessels were identified as clusters within the size range of 500–1500 μm^2 [21,22] counted and expressed as the average number of vessels per frame. Statistical significance was analyzed using a one-way ANOVA (GraphPad Prism) relative to untreated control.

3. Results

3.1. Endothelial cell migration and proliferation assay

The dECM biomaterials were mainly insoluble, so aqueous-soluble extracts were first prepared from the biomaterials prior to testing. Protein concentrations of the extracts are given in Fig. 1 (brackets) and reflect differences in the availability of soluble protein components between the biomaterials. For example, extracts of OFM and SIS prepared at 100 mg/mL gave extracts with protein concentrations of 0.8 mg/mL and 0.7 mg/mL, while the extraction of OFM-X and PG under identical conditions gave significantly more dilute protein solutions (0.3 mg/mL and 0.1 mg/mL, respectively). Comparison between the four biomaterials by normalizing to the protein concentrations of the extracts was not attempted, instead bioactivity was compared based on the mass of biomaterial extracted. In this way, the assays compared the biomaterials under more physiologically relevant conditions, assuming that a single application of each biomaterial would have a comparable mass. $VEGF_{121}$-treated cells demonstrated a statistically significant ($P < 0.001$) increase in the total cell monolayer after 4 and 8 h incubation, due to cell migration and proliferation into the denuded area. Representative images of the denuded cell monolayer treated with either PBS or OFM extract (0.8 mg/mL) at 8 h are shown in Fig. 1A and B, respectively. OFM extracts prepared at 50 or 100 mg/mL gave a statistically significant increase ($P < 0.001$) in cell migration and proliferation, relative to PBS-treated controls (Fig. 1C). Extracts of powdered SIS were less bioactive, with a statistical difference ($P < 0.05$) between PBS-treated controls and the SIS extract prepared at 100 mg/mL only. Extracts prepared from OFM-X or PG failed to elicit a statistically significant bioactivity compared to PBS.

To determine the effect of test samples on migration alone, cell proliferation was inhibited with mitomycin C prior to denuding the monolayer. Representative images of scratched monolayers incubated for 8 h with either PBS, or an OFM extract (100 mg/mL) are shown in Fig. 2A and B, respectively. OFM extracts (50 mg/mL or 100 mg/mL) stimulated cellular migration that resulted in a statistically significant increase in the total area of the cell monolayer, relative to PBS-treated controls (Fig. 2C). For example, the OFM extract prepared at 100 mg/mL exhibited a ten-fold increase in the area of the cell monolayer compared with PBS-treated control wells. Extracts prepared with powdered SIS elicited a significant bioactive response relative to control wells, but only after 8 h incubation. The bioactivity of the OFM-X and PG extracts was markedly less than that of the OFM and SIS extracts. Cellular migration in the presence of $VEGF_{121}$ was statistically significant relative to PBS-treated controls ($P < 0.001$).

3.2. Aortic ring assay

Intact OFM biomaterial and OFM aqueous-soluble components were tested using the *ex vivo* aortic ring assay. Sterile OFM powder (0.02% w/v) embedded within the fibrin gel promoted formation of microvessels extending from the aortic ring (Fig. 3B). Over 7 days, the microvasculature exhibited branching, anastomosis and lumen formation consistent with previous findings [23]. The area of microvasculature in response to the OFM biomaterial was increased at days 3 ($8.19 \times 10^5 \pm 1.00 \times 10^5$ pixels, $p < 0.05$), 5 ($1.38 \times 10^6 \pm 0.87 \times 10^5$ pixels; $p < 0.001$) and 7 ($1.49 \times 10^6 \pm 0.15 \times 10^6$ pixels; $P < 0.001$); (Fig. 3E), relative to untreated controls. In another approach, soluble components of the OFM biomaterial were extracted into MCDB-131 media, and then the media used to create the fibrin gel. In this way, aqueous-soluble OFM components would be liberated from the matrix and incorporated directly into the clot. The concentration of soluble OFM protein components incorporated into the clot was approximately 0.03 mg/mL. Aortas exposed to OFM extractables showed a statistically significant increase in microvasculature relative to untreated aortas at day 5 ($1.24 \times 10^6 \pm 0.18 \times 10^5$ pixels, $p < 0.001$) and day 7 ($1.33 \times 10^6 \pm 0.56 \times 10^5$ pixels, $p < 0.001$); (Fig. 3E).

3.3. Chicken CAM assay

Images of the *ex ovo* CAM prior to and following exposure to the extract were used to quantify changes to the vascular network in response to extractables contained in OFM, SIS, PG and OFM-X. The vascular network of the CAM at the time of dosing appeared as a robust capillary network with well established primary vessels and secondary vessels which matured and branched over time with no sign of regression during the course of the assay. A representative image of a section of CAM treated with an OFM extract, prepared at 100 mg/mL is shown in Fig. 4A and B. Raw image files were digitally deconvoluted to separate the red blood vessels from the background color channels and the total blood vessel area quantified in the resultant images (Fig. 4C and D). This allowed changes in both the relative size and number of blood vessels to be quantified in each treatment group. As expected, dosing the CAM

Fig. 4. Bioactivity of biomaterials extracts in an *ex ovo* CAM assay. A. Representative image of the CAM assay following treatment with OFM extract (0.8 mg/mL) day 0. B. Representative image of the CAM assay following treatment with OFM extract (0.8 mg/mL) day 3. Black dots indicate position of branch points for branch point analysis. C, D. Masks of images A and B following deconvolution of the color channels. E. Quantification of the percentage increase in the total blood vessel area, relative to day 0. F. Quantification of the percentage increase in the number of blood vessel branch points relative to day 0. Concentration indicated is protein concentration of extract before 20 μL added to PTFE rings. Error bars represent SEM from triplicate experiments. '*', '**' and '***' = $P < 0.05$, $P < 0.01$ and $P < 0.001$ respectively, using two-way ANOVA and Bonferroni post-hoc tests relative to the untreated controls.

with $VEGF_{121}$ resulted in a significant increase ($P < 0.001$) in blood vessel area and the number of vessel branch points at days 1, 2 and 3, compared to PBS-treated controls (Fig. 4E). Dosing with the OFM extract gave a significant increase ($P < 0.001$) in blood vessel area at all time points, relative to PBS-treated controls. For example, there was a 50.7 ± 2.0% increase in the total blood vessel area following three days incubation of the CAM with an OFM extract prepared at 100 mg/mL (Fig. 4E). The OFM extractables additionally increased in a dose-dependent manner the number of blood vessel branch points relative to a PBS-treated membrane (Fig. 4D). OFM-X failed to increase either the area of vascularization or branch points in the CAM model. PG also failed to increase area of vascularization yet the average number of branch points increased compared to PBS at 48 and 72 h ($P < 0.01$) (Fig. 4).

3.4. *In vivo pathology*

On days 14 and 28 post-wounding both control and treated wound beds were filled by granulation tissue (Fig. 5). The presence of either OFM or SIS biomaterial elicited a foreign body-type inflammatory response that decreased over time as biomaterials were incorporated. Residual fragments of either biomaterial were surrounded by low to moderate numbers of degenerate neutrophils and plaques of multinucleate giant cells (MNGCs). Surrounding these were loose layers of epithelioid macrophages and lymphocytes. If fragments were small or well degraded, MNGCs were outnumbered by epithelioid macrophages and lymphocytic cuffs were thicker and denser, sometimes forming nodules with active germinal centres. By day 42 all wounds were fully reepithelialized (Fig. 5). Newly formed epithelium was 1.5–3 times the thickness of unwounded epidermis but otherwise normal. The stratum corneum was 2–3 times thicker than that of unwounded epidermis. Residual biomaterial fragments were not present in any section. Regenerating collagen bundles of OFM and SIS-treated wounds were indistinguishable from each other and from those of control wounds.

3.5. *Quantitative assessment of in vivo angiogenesis*

Immunohistochemistry and digital quantification methods were used to quantify the development of vasculature in the neodermis following treatment with either OFM or SIS. Blood vessels were identified as endothelial cell clusters stained using a CD34 marker and a DAB chromogen (Fig. 6A). Using ImageJ, blood vessels were selected based on colour intensity and a binary mask was produced (Fig. 6B). Blood vessels in the granulation tissue were counted and expressed as the average number of blood vessels per frame within the granulation tissue (Fig. 6C). There was a statistically significant increase in the number of blood vessels in wounds treated with OFM at days 14, 28 and 42 ($P < 0.01$ at all time points), relative to untreated wounds, and the number if blood vessels in OFM-treated wounds was also significantly increased from those blood vessels counted in SIS-treated wounds ($P < 0.01$ at day 14, 28 and 42). Vessels within the granulation tissue of the excisional wounds treated with OFM were observed to have patent lumens from day 14 with plump endothelial cell linings similar to those of untreated wounds. Up until day 28 the blood vessels near the epithelial junction lay parallel to the epidermis in a tortuous fashion. In contrast, blood vessels were more random and in a diffuse pattern at day 42. Regression of the blood vessels was observed in untreated wounds and SIS-treated wounds between day 14 and day 28 whereas OFM-treated wounds did not exhibit significant regression. In SIS-treated wounds, vessels were of similar size and orientation to those wounds treated with OFM. The vessels in SIS-treated wounds showed similar patency as that seen in OFM-treated wounds but SIS treatment did not significantly increase the total number of blood vessels relative to the untreated wounds ($P > 0.05$).

4. Discussion

The supply of oxygen required for cell proliferation during tissue regeneration is limited to a diffusion distance of approximately 150 μm from the vasculature [24]. Therefore, the long-term success of dECM-based biomaterials as templates for tissue regeneration depends on adequate vascularization of the material to deliver oxygen and nutrients and allow cellular infiltration [1]. We have interrogated the angiogenicity of the OFM biomaterial using a panel of established *in vitro* and *in vivo* models and made comparisons to a clinically established dECM biomaterial, a chemically cross linked dECM and a commercially available collagen-containing wound dressing. Models were selected to best examine the angiogenic potential of the test articles and allow quantification of endothelial cell migration, proliferation, capillary sprouting and *in vivo* angiogenesis. Aqueous-soluble components of OFM stimulated proliferation and migration of HUVEC cells, and OFM extracts were more bioactive than extracts of SIS prepared under identical conditions. OFM-X and PG failed to elicit any statistical increase in proliferation or migration of HUVEC cells. The endothelial cell migration assay has previously been used to demonstrate the mitogenic and chemotactic effects of SIS extracts prepared either by extraction of SIS into basal media [25], or isolation of low molecular weight extractables following acid-hydrolysis of SIS [26]. That the stimulatory effect of OFM is greater than SIS suggests that either the relative concentration of bioactive species is higher in OFM, and/or that the proportion of macromolecules retained in a bioactive conformation is greater in OFM. Capillary outgrowth, a true measure of angiogenesis, was demonstrated in response to OFM extractables in the aortic ring and *ex ovo* CAM models. Extracts from PG failed to elicit angiogenic activity in any of the assays. The PG wound dressing is composed of 55% reconstituted collagen and 45% oxidized regenerated cellulose and therefore would not be expected to elicit a bioactive response in the assays described. The *in vivo* vascularization and remodeling resulting from cross linked dECM biomaterials has been shown to be reduced relative to non-covalently modified dECM biomaterials [27]. Our own cross linked material, OFM-X, failed to stimulate either HUVEC cell migration or the development of vasculature in the CAM model. The lack of bioactivity associated with cross linked dECM biomaterials may be due the covalent modification of important epitopes, the resistance of the biomaterial to degradation and hence liberation of matricryptic peptides, or a low abundance of soluble growth factors.

While the CAM model is useful in evaluating angiogenic extracts, it is based on an avian system which may not extrapolate to mammalian angiogenesis [28]. To address this, the angiogenicity of OFM was quantified using an *in vivo* mammalian model of tissue regeneration. In the porcine full-thickness excisional model, neither OFM nor SIS increased the rates of wound closure, consistent with previous studies of dECM-based biomaterials in acute dermal models [29]. The usefulness of these acute models is in understanding the effects on test materials during regeneration of normal tissues, rather than assessing relative wound healing rates, where more clinically relevant *in vivo* models, for example infected chronic wound models and models of compromised vascular supply (e.g. ischemic flap) may be more suitable. Within the granulation tissue, OFM-treated wounds demonstrated increased vasculature compared to SIS-treated and untreated wounds. Cells such as neutrophils, lymphocytes, eosinophils and MNGC have previously been reported in association with dECM biomaterials, a finding that is consistent with our own [29], and also consistent

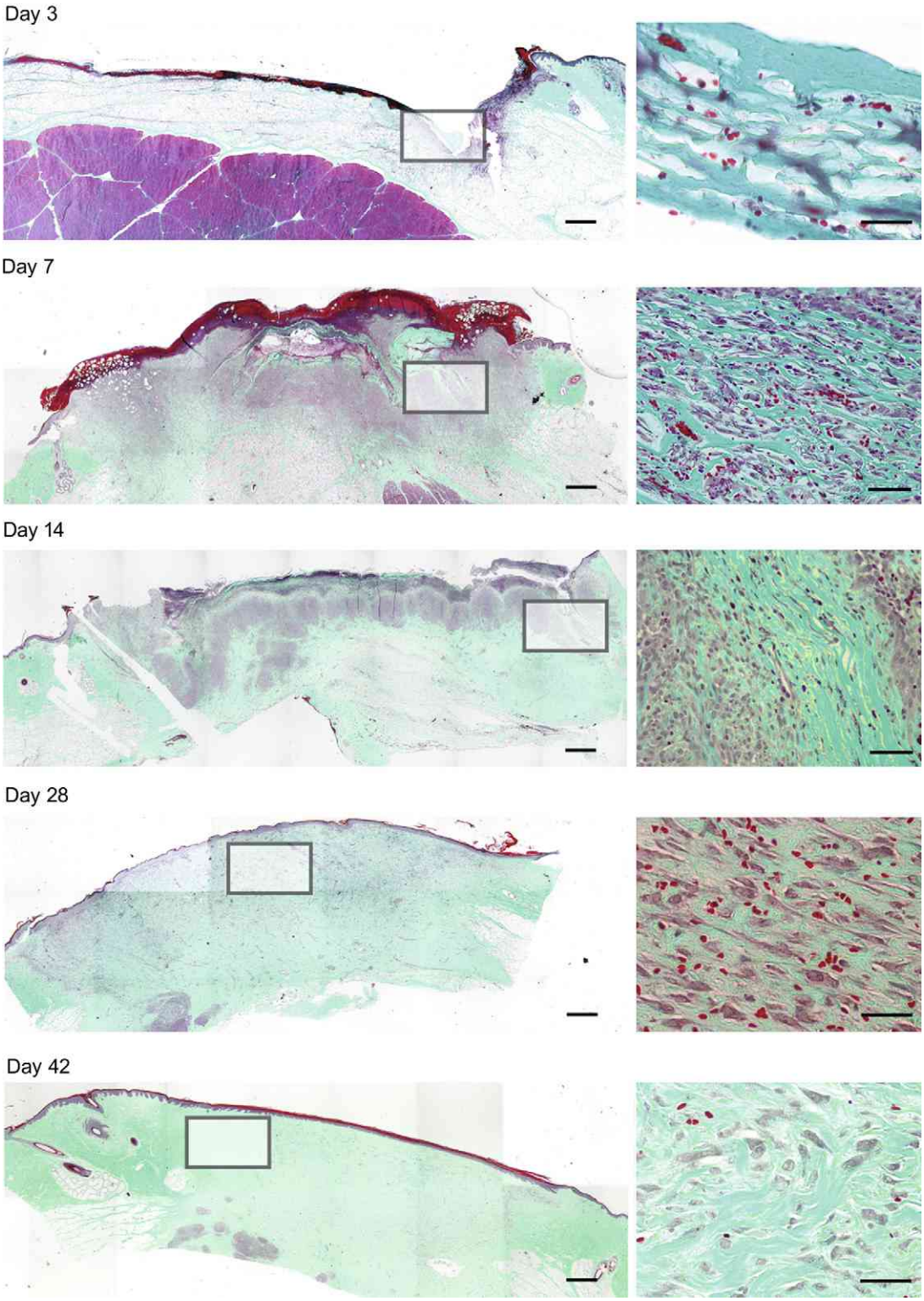

Fig. 5. Histological examination of OFM-treated wounds. Wounds were biopsied on days 7, 14, and 42, formalin-fixed, sectioned and stained with Gomori's trichrome stain (red = cytoplasm, green = collagen, blue/black = nuclei). Slides were imaged and stitched to create a whole wound image. Scale bar = 2 mm. Higher magnifications are taken in the area outlined. Scale bar = 100 μm.

with constructive remodeling of absorbable biomaterials [30]. Importantly, the inflammatory response observed in both OFM and SIS groups returned to baseline by day 42, and histologically could not be distinguished from untreated wounds. Results obtained from the *in vivo* porcine model married with those obtained from HUVEC migration/proliferation, aortic ring and CAM assay, and collectively these results support the angiogenic properties of the OFM biomaterial. That OFM stimulated the many processes leading to a robust blood supply, including cell migration, proliferation and vessel branching, suggests this biomaterial may prove to be effective in wounds with compromised blood supply, for example chronic diabetic and venous ulcers.

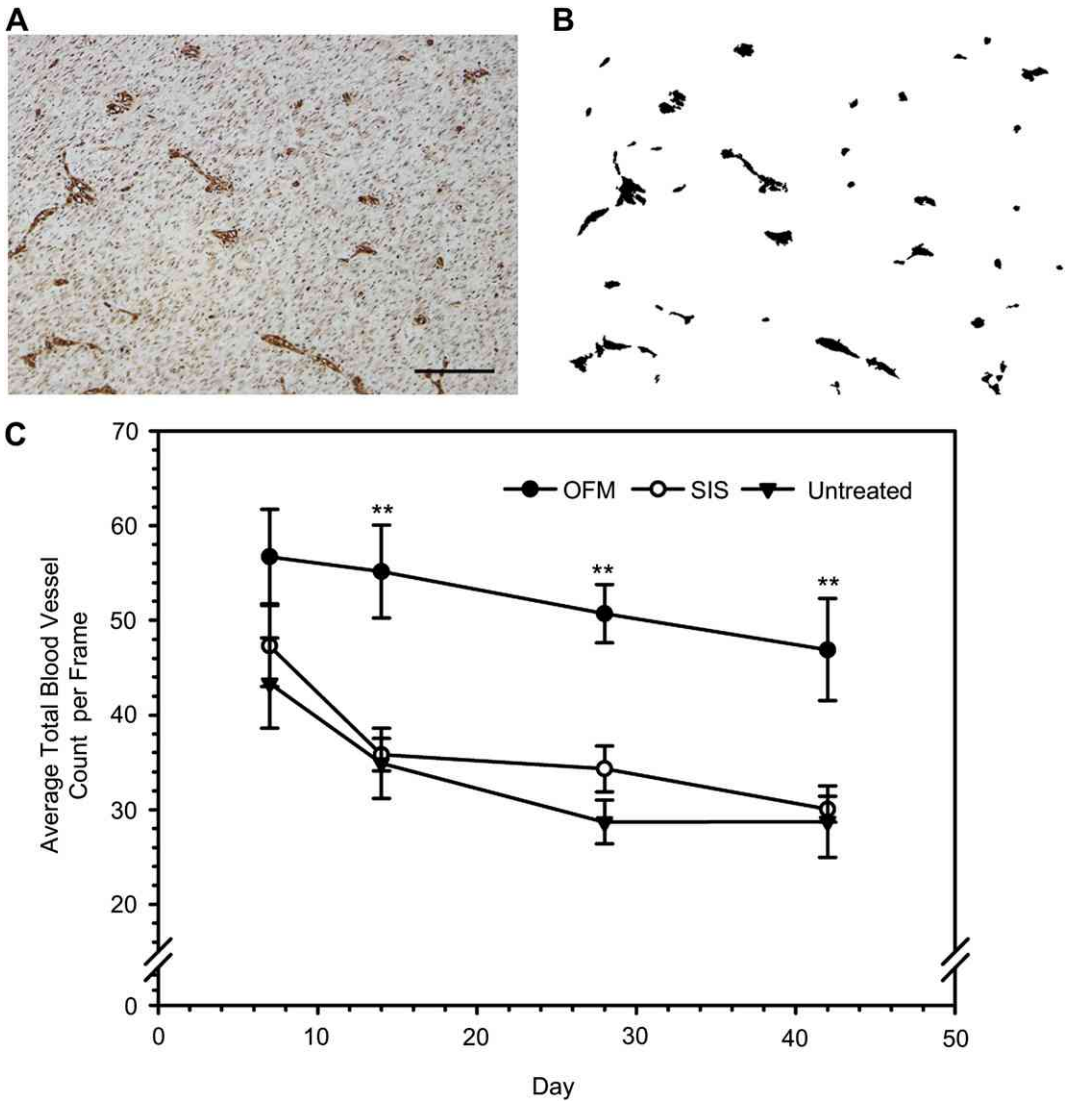

Fig. 6. Quantification of blood vessels during dermal regeneration. A. Representative image of CD34-stained tissue section. B. A representative mask of the same CD34-stained image generated using ImageJ and used to quantify the number of CD34-positve blood vessels. Scale bar = 100 μm. C. The total number of CD34-positive vessels in four frames taken from the regenerating dermal layer were quantified using IHC and digital methods. Each of the three treatment groups were sampled at the days indicated. Error bars represent SEM ($n = 5$). '**' = $P < 0.01$ significance relative to untreated control.

The ability of OFM to stimulate endothelial cell migration, proliferation and capillary formation is likely, at least in part, to be due to the availability of soluble bioactive growth factors that exert their effect either independently, or in concert. Related dECM biomaterials are known to contain various bioactive growth factors including transforming growth factor (TGF)-β [12,13], VEGF [10], and FGF2 [11,13]. Studies have demonstrated that the availability of bioactive growth factors in dECM-based biomaterials is dependent on the processing methods [31], and it is known that the component growth factors are relatively shelf-stable in a lyophilized form [11]. OFM is known to contain bioactive FGF2 that stimulates differentiation of PC12 cells *in vitro* [8]. FGF2 has been shown to encourage vasculogenesis through activation of the renin-angiotensin system [32], and via the recruitment of endothelial progenitor cells [33]. Based on the composition of related dECM-based materials such as SIS, and the close association between stimulatory macromolecules and ECM in tissues, we would expect that OFM would contain a diverse range of potentially stimulatory components in addition to FGF2. For example, we have previously shown that OFM contains HA [8], which is known to be hydrolyzed in injured tissues leading to the production of low molecule weight and highly bioactive oligomers [34]. HA oligomers stimulate endothelial cell proliferation and migration, leading to blood vessel development [34–36].

OFM was shown to be degraded and remodeled in *vivo*, resulting in organized tissues with an increased blood vessel density within the granulation tissue. While this effect may be attributed to the presence of stimulatory growth factors or glycosaminoglycans present in the biomaterial, matricryptic peptides from the enzymatic remodeling of the biomaterial may also contribute to the observed bioactivity. For example, degradation of dECM biomaterials results in low molecular weight peptides which stimulate endothelial cell migration and proliferation [15,26], and chemotaxis of endothelial progenitor cells *in vitro* [14] and *in vivo* [37]. The presence of endothelial progenitor cells leads to both angiogenesis and vasculogenesis in regenerating tissue and improved wound healing outcomes [38,39]. It is important to note that this study identified vasculature within the porcine excisional wound model and attributes this to angiogenesis however the contribution of vasculogenesis to the results obtained cannot be ruled out.

5. Conclusion

Using established quantitative methods, OFM was shown to promote endothelial cell proliferation, migration and capillary growth *in vitro* and increase blood vessel density *in vivo*. Furthermore, OFM performed better *in vitro* than SIS, OFM-X and PG and *in vivo* demonstrated higher angiogenic potential than SIS. Given the natural diversity of the molecular species encoded in the OFM biomaterial, further studies are warranted to identify angiogenic factors present in the material and dissect their bioactivity.

Author disclosure statement

SL, EWF, BRW and BCHM are shareholders of Mesynthes Limited.

Acknowledgments

We would like to acknowledge the Foundation for Research Science and Technology (New Zealand) (MSMA0701) for funding this project. Additional technical assistance was provided by Gribbles Pathology (Hamilton, New Zealand), Dr. Jacqui Harper (Malaghan Institute – Wellington, New Zealand), Carl Bigley (Carl and Wenfang Bigley Poultry – Wellington, New Zealand) and Lee Botes (Olympus, New Zealand).

References

[1] Laschke MW, Harder Y, Amon M, Martin I, Farhadi J, Ring A, et al. Angiogenesis in tissue engineering: breathing life into constructed tissue substitutes. Tissue Eng 2006;12:2093–104.
[2] Menon NG, Rodriguez ED, Byrnes CK, Girotto JA, Goldberg NH, Silverman RP. Revascularization of human acellular dermis in full-thickness abdominal wall reconstruction in the rabbit model. Ann Plast Surg 2003;50:523–7.
[3] Milburn ML, Holton LH, Chung TL, Li EN, Bochicchio GV, Goldberg NH, et al. Acellular dermal matrix compared with synthetic implant material for repair of ventral hernia in the setting of peri-operative staphylococcus aureus implant contamination: a rabbit model. Surg Infect (Larchmt) 2008;9:433–42.
[4] Franklin Jr ME, Trevino JM, Portillo G, Vela I, Glass JL, Gonzalez JJ. The use of porcine small intestinal submucosa as a prosthetic material for laparoscopic hernia repair in infected and potentially contaminated fields: long-term follow-up. Surg Endosc 2008;22:1941–6.
[5] Wainwright DJ. Use of an acellular allograft dermal matrix (AlloDerm) in the management of full-thickness burns. Burns 1995;21:243–8.
[6] Badylak SF. The extracellular matrix as a biologic scaffold material. Biomaterials 2007;28:3587–93.
[7] Badylak SF, Freytes DO, Gilbert TW. Extracellular matrix as a biological scaffold material: structure and function. Acta Biomater 2009;5:1–13.
[8] Lun S, Irvine SM, Johnson KD, Fisher NJ, Floden EW, Negron L, et al. A functional extracellular matrix biomaterial derived from ovine forestomach. Biomaterials 2010;31:4517–29.
[9] Badylak SF, Gilbert TW. Immune response to biologic scaffold materials. Semin Immunol 2008;20:109–16.
[10] Hodde JP, Record RD, Liang HA, Badylak SF. Vascular endothelial growth factor in porcine-derived extracellular matrix. Endothelium 2001;8:11–24.
[11] Hodde JP, Ernst DM, Hiles MC. An investigation of the long-term bioactivity of endogenous growth factor in OASIS wound matrix. J Wound Care 2005;14:23–5.
[12] McDevitt CA, Wildey GM, Cutrone RM. Transforming growth factor-beta1 in a sterilized tissue derived from the pig small intestine submucosa. J Biomed Mater Res A 2003;67:637–40.
[13] Voytik-Harbin SL, Brightman AO, Kraine MR, Waisner B, Badylak SF. Identification of extractable growth factors from small intestinal submucosa. J Cell Biochem 1997;67:478–91.
[14] Beattie AJ, Gilbert TW, Guyot JP, Yates AJ, Badylak SF. Chemoattraction of progenitor cells by remodeling extracellular matrix scaffolds. Tissue Eng Part A 2009;15:1119–25.
[15] Reing JE, Zhang L, Myers-Irvin J, Cordero KE, Freytes DO, Heber-Katz E, et al. Degradation products of extracellular matrix affect cell migration and proliferation. Tissue Eng Part A 2009;15:605–14.
[16] Floden EW, Malak SF, Basil-Jones MM, Negron L, Fisher JN, Lun S, et al. Biophysical characterization of ovine forestomach extracellular matrix biomaterials. J Biomed Mater Res B Appl Biomater 2010;96:67–75.
[17] Jaffe EA, Nachman RL, Becker CG, Minick CR. Culture of human endothelial cells derived from umbilical veins. Identification by morphologic and immunologic criteria. J Clin Invest 1973;52:2745–56.
[18] Franchitto A, Pichierri P, Mosesso P, Palitti F. Caffeine effect on the mitotic delay induced by G2 treatment with UVC or mitomycin C. Mutagenesis 1998;13:499–505.
[19] Nicosia RF, Ottinetti A. Growth of microvessels in serum-free matrix culture of rat aorta. A quantitative assay of angiogenesis in vitro. Lab Invest 1990;63:115–22.
[20] Prophet EB. Laboratory methods in histotechnology. Washington, D.C.: American Registry of Pathology; 1994.
[21] Meyer W, Kacza J, Zschemisch NH, Godynicki S, Seeger J. Observations on the actual structural conditions in the stratum superficiale dermidis of porcine ear skin, with special reference to its use as model for human skin. Ann Anat 2007;189:143–56.
[22] Yen A, Braverman IM. Ultrastructure of the human dermal microcirculation: the horizontal plexus of the papillary dermis. J Invest Dermatol 1976;66:131–42.
[23] Nicosia RF, Villaschi S. Rat aortic smooth muscle cells become pericytes during angiogenesis in vitro. Lab Invest 1995;73:658–66.
[24] Colton CK. Implantable biohybrid artificial organs. Cell Transplant 1995;4:415–36.
[25] Yang B, Zhou L, Sun Z, Yang R, Chen Y, Dai Y. In vitro evaluation of the bioactive factors preserved in porcine small intestinal submucosa through cellular biological approaches. J Biomed Mater Res A 2010;93:1100–9.
[26] Li F, Li W, Johnson S, Ingram D, Yoder M, Badylak S. Low-molecular-weight peptides derived from extracellular matrix as chemoattractants for primary endothelial cells. Endothelium 2004;11:199–206.
[27] Petter-Puchner AH, Fortelny RH, Walder N, Mittermayr R, Ohlinger W, van Griensven M, et al. Adverse effects associated with the use of porcine cross-linked collagen implants in an experimental model of incisional hernia repair. J Surg Res 2008;145:105–10.
[28] Auerbach R, Lewis R, Shinners B, Kubai L, Akhtar N. Angiogenesis assays: a critical overview. Clin Chem 2003;49:32–40.
[29] Prevel CD, Eppley BL, Summerlin DJ, Sidner R, Jackson JR, McCarty M, et al. Small intestinal submucosa: utilization as a wound dressing in full-thickness rodent wounds. Ann Plast Surg 1995;35:381–8.
[30] Anderson JM, Rodriguez A, Chang DT. Foreign body reaction to biomaterials. Semin Immunol 2008;20:86–100.
[31] Hodde J, Hiles M. Bioactive FGF-2 in sterilized extracellular matrix. Wounds 2001;13:195–201.
[32] D'Angelo G, Struman I, Martial J, Weiner RI. Activation of mitogen-activated protein kinases by vascular endothelial growth factor and basic fibroblast growth factor in capillary endothelial cells is inhibited by the antiangiogenic factor 16-kDa N-terminal fragment of prolactin. Proc Natl Acad Sci U S A 1995;92:6374–8.
[33] Tepper OM, Capla JM, Galiano RD, Ceradini DJ, Callaghan MJ, Kleinman ME, et al. Adult vasculogenesis occurs through in situ recruitment, proliferation, and tubulization of circulating bone marrow-derived cells. Blood 2005;105:1068–77.
[34] Slevin M, West D, Kumar P, Rooney P, Kumar S. Hyaluronan, angiogenesis and malignant disease. Int J Cancer 2004;109:793–4. author reply 5–6.
[35] Gao F, Liu Y, He Y, Yang C, Wang Y, Shi X, et al. Hyaluronan oligosaccharides promote excisional wound healing through enhanced angiogenesis. Matrix Biol 2010;29:107–16.
[36] West DC, Hampson IN, Arnold F, Kumar S. Angiogenesis induced by degradation products of hyaluronic acid. Science 1985;228:1324–6.
[37] Agrawal V, Johnson SA, Reing J, Zhang L, Tottey S, Wang G, et al. Epimorphic regeneration approach to tissue replacement in adult mammals. Proc Natl Acad Sci U S A 2010;107:3351–5.
[38] Shepherd BR, Enis DR, Wang F, Suarez Y, Pober JS, Schechner JS. Vascularization and engraftment of a human skin substitute using circulating progenitor cell-derived endothelial cells. FASEB J 2006;20:1739–41.
[39] Suh W, Kim KL, Kim JM, Shin IS, Lee YS, Lee JY, et al. Transplantation of endothelial progenitor cells accelerates dermal wound healing with increased recruitment of monocytes/macrophages and neovascularization. Stem Cells 2005;23:1571–8.